ACS OMEGA

http://pubs.acs.org/journal/acsodf

Article

Optical Characterization of Few-Layer $PtSe_2$ Nanosheet Films

Lenka Pribusová Slušná,* Tatiana Vojteková, Jana Hrdá, Helena Pálková, Peter Siffalovic, Michaela Sojková, Karol Végsö, Peter Hutár, Edmund Dobročka, Marián Varga, and Martin Hulman*

Cite This: *ACS Omega* 2021, 6, 35398−35403

Read Online

ACCESS | Metrics & More | Article Recommendations | Supporting Information

ABSTRACT: Thin films of transition-metal dichalcogenides are potential materials for optoelectronic applications. However, the application of these materials in practice requires knowledge of their fundamental optical properties. Many existing methods determine optical constants using predefined models. Here, a different approach was used. We determine the sheet conductance and absorption coefficient of few-layer $PtSe_2$ in the infrared and UV−vis ranges without recourse to any particular model for the optical constants. $PtSe_2$ samples with a thickness of about 3−4 layers were prepared by selenization of 0.5 nm thick platinum films on sapphire substrates at different temperatures. Differential reflectance was extracted from transmittance and reflectance measurements from the front and back of the sample. The film thickness, limited to a few atomic layers, allowed a thin-film approximation to calculate the optical conductance and absorption coefficient. The former has a very different energy dependence in the infrared, near-infrared, and visible ranges. The absorption coefficient exhibits a strong power-law dependence on energy with an exponent larger than three in the mid-infrared and near-infrared regions. We have not observed any evidence for a band gap in $PtSe_2$ thin layers down to an energy of 0.4 eV from our optical measurements.

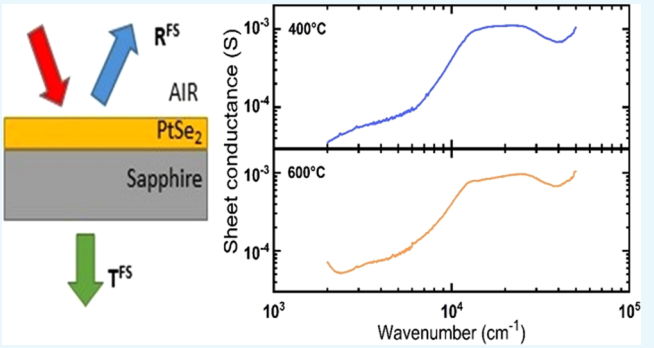

1. INTRODUCTION

Two-dimensional (2D) materials are at the center of interest due to their unique optical and electronic properties. Transition-metal dichalcogenides (TMDs) are 2D compounds with a layered structure.[1] Platinum diselenide films ($PtSe_2$), like other materials in this family, have tunable properties based on film thickness (number of monolayers). For example, the MoS_2 monolayer has a much higher photoluminescence intensity than the bulk.[2] TMD materials have the potential of being used in different device applications in electronics (transistors),[3] optoelectronics (photodetectors, sensors),[4] and ultrafast photonics (saturable absorber).[5,6] For the practical use of TMD materials in these applications, it is necessary to know the optical properties of thin films.

The optical properties of any material are entirely determined by establishing optical constants such as refractive indices, dielectric function, absorption coefficient, or optical conductivity.[7,8] The experimental methods used to determine thin films' optical constants of TMD materials include ellipsometry, Kramers−Kronig (KK)-related methods, or differential reflectivity (DR) measurements. For ellipsometry, model dielectric functions are needed to fit the experimental spectra and obtain the optical constants.[9] A similar situation occurs when reflectivity spectra are analyzed by methods using a KK transformation.[10,11] Alternatively, a differential reflectance (DR) measurement is used to obtain information on the TMD's optical properties. This method is commonly used to extract the absorption coefficient by measuring the DR in a confocal microscope of a thin film deposited on a transparent substrate.[12−14] However, the formula linking the DR and absorption coefficient was initially derived for a thin film deposited on a semi-infinite substrate.[15] In addition, considering what effect the reflection from the backside of the substrate might have, or why this reflection can be assumed insignificant, requires further assumptions or experimental evidence.[16,17]

Here, we adopt an experimental approach following more closely the original idea of McIntyre and Aspnes.[15] As a result, the imaginary part of a $PtSe_2$ thin film's dielectric function is calculated from a DR measurement without assuming any explicit model of the material's dielectric function. Such a calculation is based on a thin-film approximation in a two-phase system with a planar interface consisting of a thin film deposited on a transparent substrate and facing an ambient phase (air). The substrate is considered to be semi-infinite.

Received: August 31, 2021
Accepted: November 30, 2021
Published: December 14, 2021

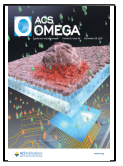

https://doi.org/10.1021/acsomega.1c04768
ACS Omega 2021, 6, 35398−35403

The theory provides an experimental test to justify the thin-film approximation. For that, a sample must be measured from the front side (FS) (incoming light beam hits the thin layer first) and from the backside. While it is difficult to do that when measuring the sample under a confocal microscope, it can be easily performed when using large-area samples and conventional spectrometers, as we did in our work. The issue with the finite thickness of a substrate is naturally solved because analytical expressions transform the as-measured transmittance and reflectance to those defined for a semi-infinite substrate. The characterization of CdTe and a-Si thin films from the experimental transmittance and back reflectance measurements was previously described with results supported by theoretical calculations.[18]

In this paper, large-area, few-layer $PtSe_2$ films were prepared on the top surface of double-side polished sapphire substrates by selenizing Pt films with a thickness of 0.5 nm and an area of ~1 cm^2. The final thickness of $PtSe_2$ layers was slightly below 2 nm as measured by X-ray reflectivity. Front side and backside transmittance and reflectance were measured in the spectral range of 200−5000 nm on grating and Fourier transform spectrometers. As-measured quantities were transformed into the reflectance and transmittance of a thin layer on a semi-infinite substrate. From the latter, the differential reflectance and the optical conductance are calculated in a thin-film approximation. In addition, the experimental approach chosen also enabled us to calculate the absorption coefficient for the few-layer $PtSe_2$ samples. We are not aware of the determination of optical properties of any other 2D-TMD material that would be performed similarly.

For completeness, we mention that the refractive indices of few-layer $PtSe_2$ films were measured in the visible and near-infrared ranges by spectroscopic ellipsometry. They were found to be strongly thickness-dependent when the thickness was less than 10 nm. The real part of the refractive index increases toward the near-infrared and then remains essentially constant up to 1600 nm. The extinction coefficient is flat in the visible region and decreases in the near-infrared region.[19−22]

2. RESULTS AND DISCUSSION

The thickness of the $PtSe_2$ layers was determined by measuring the layers' X-ray reflectivity (XRR).[23] The shape of an interference pattern of the X-ray beams reflected from the upper and bottom surfaces of the layer depends sensitively on the layer thickness. The fits to the XRR patterns gave thicknesses of 1.8 and 1.9 nm with a roughness of 0.3 nm for both samples.

The morphology of the layers was investigated by atomic force microscopy (AFM) measurements. They revealed that the layers are continuous and free of voids and isolated islands. We suppose that the thin layers coat almost the whole surface of the sapphire substrate with a size of 1 × 1 cm^2.

We also measured grazing-incidence wide-angle X-ray scattering (GIWAXS) to specify the alignment of the $PtSe_2$ layers with respect to the substrate. The results confirmed the parallel orientation of $PtSe_2$ basal planes to the substrate. The details on AFM, XRR, and GIWAXS measurements and their results are given in the Supporting Information.

Raman spectra of the samples prepared at two different temperatures were measured to confirm the presence of $PtSe_2$ (see Figure 1). The Raman peak at 178 cm^{-1} originates from a doubly degenerated in-plane vibration assigned to the E_{2g} irreducible representation of a $PtSe_2$ point group. Similarly,

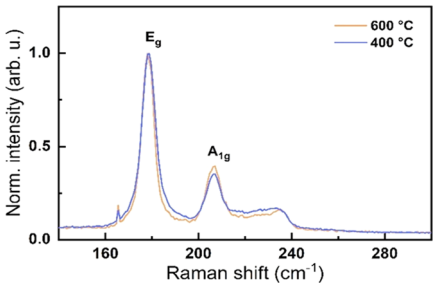

Figure 1. Normalized Raman spectra of $PtSe_2$ layers prepared at 400 °C (blue line) and 600 °C (orange line).

the line at 207 cm^{-1} is a totally symmetric A_{1g} mode with the selenium atoms vibrating out of the plane. The feature at 237 cm^{-1} is assigned to an overlap between the A_{2u} and E_u modes.[24] The spectra normalized to the intensity of the E_{2g} peak are almost identical, indicating that the growth temperature has no significant influence on the vibrational properties of the thin $PtSe_2$ layers. The intensity ratio of the two modes suggests that the layer thickness is less than 2 nm, in agreement with the XRR measurements.[25]

Reflectance and transmittance spectra measured from 2000 to 50 000 cm^{-1} are shown in Figure 2 for $PtSe_2$ samples. The

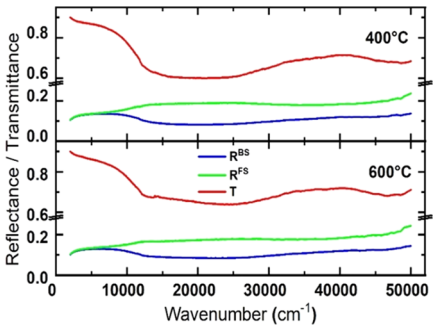

Figure 2. Front side (green line) and backside (blue line) reflectance spectra of $PtSe_2$ samples grown at indicated temperatures. The transmittance spectra (red line) are mean values calculated from the front side and backside measurements.

transmittance spectra measured for the two sample orientations, i.e., either front side (FS) with the few-layer film or backside (BS) to the incident beam, are the same within the measurement error. This is consistent with the theoretical prediction and is used to verify the accuracy of the measurements. Therefore, these spectra are averaged in Figure 2.

The transmittance spectra show a broad maximum and minimum in the visible region and increase toward the infrared region. Reflectance spectra from the front side (R^{FS}, green line) and backside (R^{BS}, blue line) are almost featureless, and below 7000 cm^{-1}, they merge into a single spectrum.

The thin layer's optical conductance can be extracted from the DR measurements. The layer (designed as medium 2) is bound between two other media—air (medium 1) and the sapphire substrate (medium 3). McIntyre and Aspnes derived the following formula for the DR at normal incidence (see details in the Supporting Information)[15]

$$\frac{\Delta R}{R} = \frac{8\pi n_1 d}{\lambda} \frac{\varepsilon_2''}{n_3^2 - n_1^2} \quad (1)$$

https://doi.org/10.1021/acsomega.1c04768
ACS Omega 2021, 6, 35398−35403

where $n_1(=1)$ and n_3 are the refractive indices of air and sapphire, respectively, and λ is the light wavelength. ε_2'' is the imaginary part of a dielectric function and d is the layer thickness. The thin-film approximation they used to obtain eq 1 is valid for $d/\lambda \leq 0.01$. Using the formula connecting the real part of the optical conductance, σ, and ε_2'', $\sigma = \varepsilon_0 \omega \varepsilon_2''$, we obtain

$$\sigma d = \frac{\Delta R}{R} \frac{(n_3^2 - n_1^2)}{4 n_1 Z_0} \tag{2}$$

where $Z_0 = 1/\varepsilon_0 c \approx 377\ \Omega$ is the impedance of free space and ω is the circular frequency of light. The quantity σd on the lhs is the sheet conductance in the unit of siemens (Ω^{-1}).[17]

Two important points are worth mentioning. First, formulas 1 and 2 are obtained for the experimental arrangement when the light beam approaches from the front side, hitting the thin layer first and then propagating through the substrate. When the beam impinges from the backside (the substrate first and then the thin layer), the refractive indices n_1 and n_3 are interchanged in eqs 1 and 2. The backside differential reflectance (DR) becomes negative ($n_3 > n_1$), and, theoretically, the absolute magnitude of the backside DR should be by a factor of $n_3/n_1 \approx 1.7$ larger than the DR measured from the front side. On the other hand, the sheet conductance in eq 2 is a positively defined quantity with a value independent of the sample orientation.

The second remark concerns another assumption leading to eq 1, namely, the substrate is semi-infinite. This is difficult to achieve experimentally, but the as-measured reflectances R^{FS} and R^{BS} and transmittance T can be transformed analytically into reflectances R_{123} and R_{321} and transmittance T_{123} of a thin layer sandwiched between the semi-infinite substrate and air (details are explained in the Supporting Information). The order of the numbers in the subscript determines the order in which the light passes through the structure (for instance, 123 means air → thin layer → substrate). Two differential reflectances, one for the measurement from the front side and the other measured from the sample rear, are defined as follows

$$\left(\frac{\Delta R}{R}\right)^{FS} = \frac{R_{123} - R_{13}}{R_{13}} \tag{3}$$

$$\left(\frac{\Delta R}{R}\right)^{BS} = \frac{R_{321} - R_{31}}{R_{31}} \tag{4}$$

where $R_{13} = R_{31}$ is the reflectance of an air−sapphire interface. The latter is related to the experimentally measured reflectance R_{slab} of a sapphire substrate by $R_{13} = \frac{R_{slab}}{2 - R_{slab}}$.[8] It is assumed that the absorption of the sapphire substrate is negligible.

The front side and backside DRs calculated using eqs 3 and 4 are shown in Figure 3 for $PtSe_2$ samples selenized at two different temperatures. By inspection, we see that the backside DRs are indeed negative in the entire spectral range investigated. However, the magnitude of the backside DR is only slightly larger than that of the front side DR. The wavenumber dependence of the DR is flat in the infrared, followed by a steep increase and a weak dependence in the visible range. In the UV, the DRs' spectral dependence indicates a breakdown of the thin-film approximation. This corresponds to wavelengths below 300 nm, which no longer satisfy the assumed first-order approximation. Despite that, our

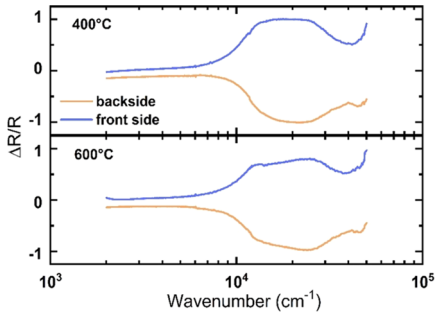

Figure 3. Differential reflectance of $PtSe_2$ samples grown at the temperatures of 400 and 600 °C. Front side and backside differential reflectances are shown as blue and orange solid lines, respectively.

measurements validate the conclusions of the McIntyre-Aspnes calculation and justify the further use of a thin-film approximation.

The optical conductance resulting from backside measurements is smaller than that from front side measurements because the magnitude of the experimentally obtained DR is smaller than that theoretically expected. The two frequency-dependent sheet conductance values obtained this way were subsequently averaged for each $PtSe_2$ sample, and the results are shown in Figure 4. Two regions "linear" in the log−log

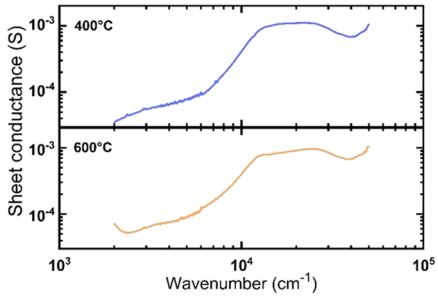

Figure 4. Optical sheet conductance of $PtSe_2$ thin films prepared at 400°C and 600°.

scale are visible in the figures. The conductance depends weakly on the frequency in the infrared range, increasing more steeply in the visible range. The two regions meet in the 6000−7000 cm^{-1} range (~0.75−0.9 eV). The sudden change in the sheet conductance can presumably indicate the onset of an electronic transition between the valence and conductance bands.

Further, in the visible range, the optical conductance is almost frequency independent. Assuming that σ follows a power-law dependence piecewise in different spectral regions, the corresponding exponents in $\sigma \sim \omega^n$ are $n < \sim 0.5$, ~2.8, and ~0 in the infrared, near-infrared, and visible range, respectively. The relation $\varepsilon_2'' \sim \omega^{n-1}$ then holds for the dielectric function, and its magnitude increases in the near-infrared region from ~7000 to ~12 000 cm^{-1} (0.9−1.5 eV) and then decreases at higher energies in the visible range. This last observation is in quantitative agreement with the frequency dependence of the imaginary part of the dielectric function obtained from ellipsometric measurements.[19−22] So far, no results regarding the optical conductance or dielectric function in the infrared range have been reported, and so no comparison of our results with others can be made. On the other hand, similar weak frequency dependence of the conductance was observed for

https://doi.org/10.1021/acsomega.1c04768
ACS Omega 2021, 6, 35398−35403

crystals of $MoTe_2$ and WTe_2 compounds hosting Weyl-type fermions.[26,27]

The weak frequency dependence in the infrared allows an approximate comparison of the sheet conductance with the values obtained from DC transport measurements. The former is in the 10−100 μS range for the two $PtSe_2$ samples. This result reasonably agrees with the DC sheet conductance of ∼10−130 μS reported in refs 23, 28, 29 for selenized layers of a similar thickness.

The electronic structure of 1T-PtSe2 is strongly layer-dependent. The monolayer is an indirect semiconductor with a calculated band gap of 1.2−1.5 eV.[30−33] The band gap rapidly decreases with increasing numbers of layers, and the samples as thick as 5−6 layers (3−4 nm) are already semimetallic. Experimentally, the band gap of $PtSe_2$ layers grown by molecular-beam epitaxy was recently measured by scanning tunneling spectroscopy (STS).[34] The values obtained from STS experiments were 0.6 eV and 0.2 eV for three and four layers, respectively, and 0 eV for layer numbers greater than five.

The band gap energy of a thin semiconducting film is often determined by measuring its absorption coefficient α. The band gap is the intersection of a linear part of a Tauc plot, $(\alpha \cdot E)^{1/\beta}$, with the energy ($E$) abscissa. For such analysis, $PtSe_2$ has been considered an indirect band gap semiconductor with $\beta = 2$.[25,35,36] The band gap extracted this way is in the range of 0.4−0.8 eV for $PtSe_2$ samples with 3−5 layers (∼2−3 nm thick).[21,25,33,35,36]

The absorption coefficient can also be evaluated within the approach presented here. In the Supporting Information, it is shown that

$$\alpha \cdot d = \ln\left(\frac{1 - R_{321}}{T_{123}}\right) \quad (5)$$

in the thin-film approximation. The result for the two $PtSe_2$ samples is displayed in Figure 5. The quantity on the ordinate is a dimensionless product of the absorption coefficient and the layer thickness.

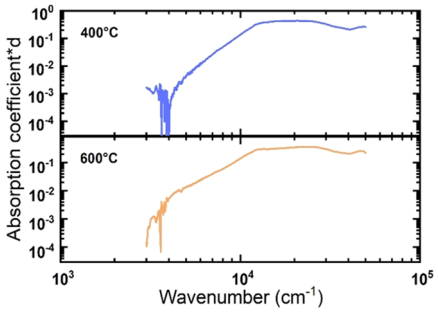

Figure 5. Spectrum of an absorption coefficient multiplied by the sample thickness d for few-layer $PtSe_2$ films prepared at 400 °C and 600 °C.

A linear part (in a log−log scale) covering almost the entire infrared and near-infrared regions dominates the absorption vs energy relation. The two spectra are quite similar, confirming the previous conclusion that the growth temperature does not alter the optical properties of few-layer $PtSe_2$ films. Taking into account the layer thickness of $\sim 2 \times 10^{-7}$ cm, the maximum absorption coefficient is of the order 10^6 cm^{-1} in the visible region of the spectrum and decreases toward the infrared range according to a power-law dependence.[19,22] The exponents of the $\alpha \sim E^m$ dependence are relatively large, with m between 3 and 4 for the two samples. The absorption coefficient has a more pronounced frequency dependence than previously reported. As a result, the Tauc plot does not have a linear part, and our $PtSe_2$ samples do not follow the behavior expected for indirect band gap semiconductors. No band gap was detected in the absorption coefficient spectrum for energies larger than ∼0.4 eV, as seen in Figure 6. This observation is in agreement with calculations predicting a vanishingly small band gap for few-layer $PtSe_2$ films.[32]

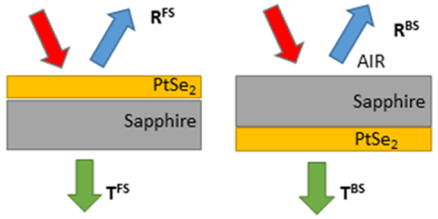

Figure 6. Scheme of the optical measurement in the front side, FS, (left) and backside, BS, (right) arrangements. R and T stand for reflectance and transmittance, respectively. A red arrow depicts the incident light.

3. CONCLUSIONS

In conclusion, we report optical measurements of large-area, few-layer $PtSe_2$ films deposited on a sapphire substrate. They were prepared by selenizing 0.5 nm thick Pt films at two growth temperatures. First, Raman scattering measurement confirmed a successful transformation of platinum into $PtSe_2$. The very small thickness of the samples allows using a thin-film approximation and calculating the frequency dependence of the differential reflectance analytically from both sides' reflection and transmission measurements. A sheet conductance was subsequently calculated from the known differential reflectance and refractive index of the sapphire substrate. The conductance's frequency dependence is weak in the infrared but becomes much steeper in the near-infrared. In the visible range, it changes only moderately again. Also, the absorption coefficient was calculated for $PtSe_2$ in the thin-film approximation. It follows a power-law dependence in the infrared and near-infrared regions with a more prominent exponent than previously reported. No band gap was detected in our samples for energies down to 0.4 eV. Our study may help better understand the electronic and optical properties of a few-layer $PtSe_2$, a promising 2D material.

4. EXPERIMENTAL SECTION

Platinum was magnetron sputtered on a c-plane double-side polished sapphire substrate to fabricate a Pt film with a thickness of 0.5 nm. Two series of Pt films were then annealed in a chemical vapor deposition (CVD) chamber with 0.1 g of 99.999% pure selenium powder at the annealing temperatures of 400 and 600 °C. Details on growth conditions and preparation methodology can be found in our previous publications on $PtSe_2$.[23,37,38]

A confocal Raman microscope (Alpha 300R, Witec, Germany) with an excitation wavelength of 532 nm was used for Raman scattering measurements. All Raman spectra were collected at room temperature using a 50× objective coupled to a 100 μm optical fiber serving as a confocal pinhole.

https://doi.org/10.1021/acsomega.1c04768
ACS Omega 2021, 6, 35398−35403

In the UV−vis range, reflectance and transmittance spectra were measured with a Shimadzu SolidSpec-3700 spectrophotometer. In the infrared region, a Fourier transform infrared spectrometer (Nicolet 6700) was used. A DTGS detector with a KBr beam splitter and an InGaS detector with a CaF_2 beam splitter were utilized in the mid-IR and near-IR ranges.

The schematic arrangement of the optical measurements is shown in Figure 6. The sample's reflectance and transmittance were measured from both the front side ($PtSe_2$ layer facing the light beam first) and the backside (with the sapphire substrate facing the beam first). The angle between the incident light and sample normal was 5° in reflectance measurements. The beam size in the UV−vis spectrometer was 2 × 4 mm^2 (width × height). Transmittance and reflectance spectra of the uncoated substrate were measured as a reference and corrected by a factor to obtain the sapphire's real refractive index, identical to that presented in ref 39. The same factor was also used to correct the as-measured reflectivity spectra of $PtSe_2$ layers. The correction factor was very close to 1 throughout the spectral range for transmittance, and so it was not assumed in the analysis. The spectra measured by two different spectrometers were eventually merged into one covering the spectral range from 2000 to 50 000 cm^{-1}.

■ ASSOCIATED CONTENT

Supporting Information

The Supporting Information is available free of charge at https://pubs.acs.org/doi/10.1021/acsomega.1c04768.

Derivation of formulas on differential conductance, sheet conductivity, and absorption coefficient; results on AFM, XRR, and GIWAXS measurements (PDF)

■ AUTHOR INFORMATION

Corresponding Authors

Lenka Pribusová Slušná − *Institute of Electrical Engineering, Slovak Academy of Sciences, 84104 Bratislava, Slovakia*; Email: lenka.pribusova-slusna@savba.sk

Martin Hulman − *Institute of Electrical Engineering, Slovak Academy of Sciences, 84104 Bratislava, Slovakia*; orcid.org/0000-0002-5598-9245; Email: martin.hulman@savba.sk

Authors

Tatiana Vojteková − *Institute of Electrical Engineering, Slovak Academy of Sciences, 84104 Bratislava, Slovakia*

Jana Hrdá − *Institute of Electrical Engineering, Slovak Academy of Sciences, 84104 Bratislava, Slovakia*

Helena Pálková − *Institute of Inorganic Chemistry, Slovak Academy of Sciences, 84536 Bratislava, Slovakia*

Peter Siffalovic − *Institute of Physics, Slovak Academy of Sciences, 84511 Bratislava, Slovakia; Centre for Advanced Materials Application, 84511 Bratislava, Slovakia*; orcid.org/0000-0002-9807-0810

Michaela Sojková − *Institute of Electrical Engineering, Slovak Academy of Sciences, 84104 Bratislava, Slovakia*; orcid.org/0000-0002-7490-3240

Karol Végsö − *Institute of Physics, Slovak Academy of Sciences, 84511 Bratislava, Slovakia*; orcid.org/0000-0003-2595-6036

Peter Hutár − *Institute of Electrical Engineering, Slovak Academy of Sciences, 84104 Bratislava, Slovakia*

Edmund Dobročka − *Institute of Electrical Engineering, Slovak Academy of Sciences, 84104 Bratislava, Slovakia*

Marián Varga − *Institute of Electrical Engineering, Slovak Academy of Sciences, 84104 Bratislava, Slovakia*

Complete contact information is available at: https://pubs.acs.org/10.1021/acsomega.1c04768

Notes

The authors declare no competing financial interest.

■ ACKNOWLEDGMENTS

This work was supported by the Slovak Research and Development Agency, projects APVV 15-0693, 19-0365, 20-0111, VEGA 2/0059/21. M.V. acknowledges project no. 19MRP0010 financed from the MoRePro Programme and funding from the Slovak Academy of Sciences.

■ REFERENCES

(1) Manzeli, S.; Ovchinnikov, D.; Pasquier, D.; Yazyev, O. V.; Kis, A. 2D Transition Metal Dichalcogenides. *Nat. Rev. Mater.* **2017**, *2*, No. 17033.

(2) Sundaram, R. S.; Engel, M.; Lombardo, A.; Krupke, R.; Ferrari, A. C.; Avouris, P.; Steiner, M. Electroluminescence in Single Layer MoS_2. *Nano Lett.* **2013**, *13*, 1416−1421.

(3) Radisavljevic, B.; Radenovic, A.; Brivio, J.; Giacometti, V.; Kis, A. Single-Layer MoS2 Transistors. *Nat. Nanotechnol.* **2011**, *6*, 147−150.

(4) Lopez-Sanchez, O.; Lembke, D.; Kayci, M.; Radenovic, A.; Kis, A. Ultrasensitive Photodetectors Based on Monolayer MoS2. *Nat. Nanotechnol.* **2013**, *8*, 497−501.

(5) Yao, Y.; Zhang, F.; Chen, B.; Zhao, Y.; Cui, N.; Sun, D.; Liu, S.; Zhang, Y.; Zhang, H.; Zhang, H. Nonlinear Optical Property and Mid-Infrared Q-Switched Laser Application at 2.8 μm of PtSe2 Material. *Opt. Laser Technol.* **2021**, *139*, No. 106983.

(6) Cheng, P. K.; Tang, C. Y.; Ahmed, S.; Qiao, J.; Zeng, L.-H.; Tsang, Y. H. Utilization of Group 10 2D TMDs-$PdSe_2$ as a Nonlinear Optical Material for Obtaining Switchable Laser Pulse Generation Modes. *Nanotechnology* **2021**, *32*, No. 055201.

(7) Dressel, M.; Grüner, G. *Electrodynamics of Solids: Optical Properties of Electrons in Matter*; Cambridge University Press: Cambridge, 2002.

(8) Stenzel, O. *The Physics of Thin Film Optical Spectra: An Introduction*; Springer Series in Surface Sciences; Springer: Berlin, New York, 2005.

(9) Azzam, R. M. A.-G.; Bashara, N. M. *Ellipsometry and Polarized Light*; North-Holland Personal Library; Elsevier: Amsterdam, 1999.

(10) Li, Y.; Chernikov, A.; Zhang, X.; Rigosi, A.; Hill, H. M.; van der Zande, A. M.; Chenet, D. A.; Shih, E.-M.; Hone, J.; Heinz, T. F. Measurement of the Optical Dielectric Function of Monolayer Transition-Metal Dichalcogenides: MoS2, MoSe2, WS2, and WSe2. *Phys. Rev. B* **2014**, *90*, No. 205422.

(11) Rigosi, A. F.; Hill, H. M.; Li, Y.; Chernikov, A.; Heinz, T. F. Probing Interlayer Interactions in Transition Metal Dichalcogenide Heterostructures by Optical Spectroscopy: MoS_2/WS_2 and $MoSe_2$/WSe_2. *Nano Lett.* **2015**, *15*, 5033−5038.

(12) Dhakal, K. P.; Duong, D. L.; Lee, J.; Nam, H.; Kim, M.; Kan, M.; Lee, Y. H.; Kim, J. Confocal Absorption Spectral Imaging of MoS_2: Optical Transitions Depending on the Atomic Thickness of Intrinsic and Chemically Doped MoS_2. *Nanoscale* **2014**, *6*, 13028−13035.

(13) Hill, H. M.; Rigosi, A. F.; Krylyuk, S.; Tian, J.; Nguyen, N. V.; Davydov, A. V.; Newell, D. B.; Hight Walker, A. R. Comprehensive Optical Characterization of Atomically Thin NbSe2. *Phys. Rev. B* **2018**, *98*, No. 165109.

(14) Zhao, W.; Ghorannevis, Z.; Chu, L.; Toh, M.; Kloc, C.; Tan, P.-H.; Eda, G. Evolution of Electronic Structure in Atomically Thin Sheets of WS_2 and WSe_2. *ACS Nano* **2013**, *7*, 791−797.

(15) McIntyre, J. D. E.; Aspnes, D. E. Differential Reflection Spectroscopy of Very Thin Surface Films. *Surf. Sci.* **1971**, *24*, 417−434.
(16) Morozov, Y. V.; Kuno, M. Optical Constants and Dynamic Conductivities of Single Layer MoS_2, $MoSe_2$, and WSe_2. *Appl. Phys. Lett.* **2015**, *107*, No. 083103.
(17) Li, Y.; Heinz, T. F. Two-Dimensional Models for the Optical Response of Thin Films. *2D Mater.* **2018**, *5*, No. 025021.
(18) Laaziz, Y.; Bennouna, A.; Chahboun, N.; Outzourhit, A.; Ameziane, E. L. Optical Characterization of Low Optical Thickness Thin Films from Transmittance and Back Reflectance Measurements. *Thin Solid Films* **2000**, *372*, 149−155.
(19) Gulo, D. P.; Yeh, H.; Chang, W.-H.; Liu, H.-L. Temperature-Dependent Optical and Vibrational Properties of PtSe2 Thin Films. *Sci. Rep.* **2020**, *10*, No. 19003.
(20) He, J.; Jiang, W.; Zhu, X.; Zhang, R.; Wang, J.; Zhu, M.; Wang, S.; Zheng, Y.; Chen, L. Optical Properties of Thickness-Controlled $PtSe_2$ Thin Films Studied *via* Spectroscopic Ellipsometry. *Phys. Chem. Chem. Phys.* **2020**, *22*, 26383−26389.
(21) Xie, J.; Zhang, D.; Yan, X.-Q.; Ren, M.; Zhao, X.; Liu, F.; Sun, R.; Li, X.; Li, Z.; Chen, S.; Liu, Z.-B.; Tian, J.-G. Optical Properties of Chemical Vapor Deposition-Grown $PtSe_2$ Characterized by Spectroscopic Ellipsometry. *2D Mater.* **2019**, *6*, No. 035011.
(22) Wang, G.; Wang, K.; McEvoy, N.; Bai, Z.; Cullen, C. P.; Murphy, C. N.; McManus, J. B.; Magan, J. J.; Smith, C. M.; Duesberg, G. S.; Kaminer, I.; Wang, J.; Blau, W. J. Ultrafast Carrier Dynamics and Bandgap Renormalization in Layered $PtSe_2$. *Small* **2019**, *15*, No. 1902728.
(23) Sojková, M.; Dobročka, E.; Hutár, P.; Tašková, V.; Pribusová Slušná, L.; Stoklas, R.; Píš, I.; Bondino, F.; Munnik, F.; Hulman, M. High Carrier Mobility Epitaxially Aligned PtSe2 Films Grown by One-Zone Selenization. *Appl. Surf. Sci.* **2021**, *538*, No. 147936.
(24) O'Brien, M.; McEvoy, N.; Motta, C.; Zheng, J.-Y.; Berner, N. C.; Kotakoski, J.; Elibol, K.; Pennycook, T. J.; Meyer, J. C.; Yim, C.; Abid, M.; Hallam, T.; Donegan, J. F.; Sanvito, S.; Duesberg, G. S. Raman Characterization of Platinum Diselenide Thin Films. *2D Mater.* **2016**, *3*, No. 021004.
(25) Chung, C.-C.; Yeh, H.; Wu, P.-H.; Lin, C.-C.; Li, C.-S.; Yeh, T.-T.; Chou, Y.; Wei, C.-Y.; Wen, C.-Y.; Chou, Y.-C.; Luo, C.-W.; Wu, C.-I.; Li, M.-Y.; Li, L.-J.; Chang, W.-H.; Chen, C.-W. Atomic-Layer Controlled Interfacial Band Engineering at Two-Dimensional Layered $PtSe_2$/Si Heterojunctions for Efficient Photoelectrochemical Hydrogen Production. *ACS Nano* **2021**, *15*, 4627−4635.
(26) Santos-Cottin, D.; Martino, E.; Le Mardelé, F.; Witteveen, C.; von Rohr, F. O.; Homes, C. C.; Rukelj, Z.; Akrap, A. Low-Energy Excitations in Type-II Weyl Semimetal Td−MoTe2 Evidenced through Optical Conductivity. *Phys. Rev. Mater.* **2020**, *4*, No. 021201.
(27) Kimura, S.; Nakajima, Y.; Mita, Z.; Jha, R.; Higashinaka, R.; Matsuda, T. D.; Aoki, Y. Optical Evidence of the Type-II Weyl Semimetals MoTe2 and WTe2. *Phys. Rev. B* **2019**, *99*, No. 195203.
(28) Urban, F.; Gity, F.; Hurley, P. K.; McEvoy, N.; Di Bartolomeo, A. Isotropic Conduction and Negative Photoconduction in Ultrathin $PtSe_2$ Films. *Appl. Phys. Lett.* **2020**, *117*, No. 193102.
(29) Yim, C.; McEvoy, N.; Riazimehr, S.; Schneider, D. S.; Gity, F.; Monaghan, S.; Hurley, P. K.; Lemme, M. C.; Duesberg, G. S. Wide Spectral Photoresponse of Layered Platinum Diselenide-Based Photodiodes. *Nano Lett.* **2018**, *18*, 1794−1800.
(30) Cao, B.; Ye, Z.; Yang, L.; Gou, L.; Wang, Z. Recent Progress in Van Der Waals 2D $PtSe_2$. *Nanotechnology* **2021**, *32*, No. 412001.
(31) Wang, G.; Wang, Z.; McEvoy, N.; Fan, P.; Blau, W. J. Layered $PtSe_2$ for Sensing, Photonic, and (Opto-)Electronic Applications. *Adv. Mater.* **2021**, *33*, No. 2004070.
(32) Ansari, L.; Monaghan, S.; McEvoy, N.; Coileáin, C. Ó.; Cullen, C. P.; Lin, J.; Siris, R.; Stimpel-Lindner, T.; Burke, K. F.; Mirabelli, G.; Duffy, R.; Caruso, E.; Nagle, R. E.; Duesberg, G. S.; Hurley, P. K.; Gity, F. Quantum Confinement-Induced Semimetal-to-Semiconductor Evolution in Large-Area Ultra-Thin PtSe2 Films Grown at 400 °C. *npj 2D Mater. Appl.* **2019**, *3*, No. 33.
(33) Wang, L.; Zhang, S.; McEvoy, N.; Sun, Y.; Huang, J.; Xie, Y.; Dong, N.; Zhang, X.; Kislyakov, I. M.; Nunzi, J.; Zhang, L.; Wang, J. Nonlinear Optical Signatures of the Transition from Semiconductor to Semimetal in $PtSe_2$. *Laser Photonics Rev.* **2019**, *13*, No. 1900052.
(34) Zhang, L.; Yang, T.; Sahdan, M. F.; Arramel; Xu, W.; Xing, K.; Feng, Y. P.; Zhang, W.; Wang, Z.; Wee, A. T. S. Precise Layer-Dependent Electronic Structure of MBE-Grown $PtSe_2$. *Adv. Electron. Mater.* **2021**, *7*, No. 2100559.
(35) Su, T.-Y.; Chen, Y.-Z.; Wang, Y.-C.; Tang, S.-Y.; Shih, Y.-C.; Cheng, F.; Wang, Z. M.; Lin, H.-N.; Chueh, Y.-L. Highly Sensitive, Selective and Stable NO_2 Gas Sensors with a Ppb-Level Detection Limit on 2D-Platinum Diselenide Films. *J. Mater. Chem. C* **2020**, *8*, 4851−4858.
(36) Shin, H. J.; Bae, S.; Sim, S. Ultrafast Auger Process in Few-Layer $PtSe_2$. *Nanoscale* **2020**, *12*, 22185−22191.
(37) Hrdá, J.; Tašková, V.; Vojteková, T.; Slušná, L. P.; Dobročka, E.; Píš, I.; Bondino, F.; Hulman, M.; Sojková, M. Tuning the Charge Carrier Mobility in Few-Layer $PtSe_2$ Films by Se: Pt Ratio. *RSC Adv.* **2021**, *11*, 27292−27297.
(38) Sojková, M.; Hrdá, J.; Volkov, S.; Vegso, K.; Shaji, A.; Vojteková, T.; Slušná, L. P.; Gál, N.; Dobročka, E.; Siffalovic, P.; Roch, T.; Gregor, M.; Hulman, M. Growth of $PtSe_2$ Few-Layer Films on NbN Superconducting Substrate. *Appl. Phys. Lett.* **2021**, *119*, No. 013101.
(39) Malitson, I. H. Refraction and Dispersion of Synthetic Sapphire. *J. Opt. Soc. Am.* **1962**, *52*, No. 1377.

https://doi.org/10.1021/acsomega.1c04768
ACS Omega 2021, 6, 35398−35403